

# Metabolic signatures of cardiorenal dysfunction in plasma from sickle cell patients as a function of therapeutic transfusion and hydroxyurea treatment

Angelo D'Alessandro,<sup>1,2</sup> S. Mehdi Nouraie,<sup>3</sup> Yingze Zhang,<sup>3</sup> Francesca Cendali,<sup>1</sup> Fabia Gamboni,<sup>1</sup> Julie A. Reisz,<sup>1</sup> Xu Zhang,<sup>4</sup> Kyle W. Bartsch,<sup>5,6</sup> Matthew D. Galbraith,<sup>5,6</sup> Joaquin M. Espinosa,<sup>5,6,7</sup> Victor R. Gordeuk<sup>4</sup> and Mark T. Gladwin<sup>8</sup>

<sup>1</sup>Department of Biochemistry and Molecular Genetics, University of Colorado Denver – Anschutz Medical Campus, Aurora, CO; <sup>2</sup>Division of Hematology, Department of Medicine, University of Colorado Denver – Anschutz Medical Campus, Aurora, CO; <sup>3</sup>Division of Pulmonary, Allergy and Critical Care Medicine, Department of Medicine, University of Pittsburgh, PE; <sup>4</sup>Department of Medicine, University of Illinois at Chicago, Chicago, IL; <sup>5</sup>Linda Crnic Institute for Down Syndrome, University of Colorado – Anschutz Medical Campus, Aurora, CO; <sup>6</sup>Department of Pharmacology, University of Colorado – Anschutz Medical Campus, Aurora, CO; <sup>7</sup>School of Medicine Information Services, University of Colorado – Anschutz Medical Campus, Aurora, CO and <sup>8</sup>University of Maryland School of Medicine, University of Maryland, Baltimore, MD, USA

**Correspondence:** A. D'Alessandro  
[angelo.dalessandro@cuanschutz.edu](mailto:angelo.dalessandro@cuanschutz.edu)

M.T. Gladwin  
[mgladwin@som.umaryland.edu](mailto:mgladwin@som.umaryland.edu)

**Received:** April 5, 2023.

**Accepted:** June 30, 2023.

**Early view:** July 13, 2023.

<https://doi.org/10.3324/haematol.2023.283288>

©2023 Ferrata Storti Foundation

Published under a CC BY-NC license



# SUPPLEMENTARY MATERIAL

## Metabolic signatures of cardiorenal dysfunction in plasma from sickle cell patients as a function of therapeutic transfusion and hydroxyurea treatment

Angelo D'Alessandro<sup>1,2,\*</sup> S. Mehdi Nouraie,<sup>3</sup> Yingze Zhang,<sup>3</sup> Francesca Cendali,<sup>1</sup> Fabia Gamboni,<sup>1</sup> Julie A. Reisz,<sup>1</sup> Xu Zhang,<sup>4</sup> Kyle W. Bartsch,<sup>5</sup> Matthew D. Galbraith,<sup>5</sup> Joaquin M. Espinosa,<sup>5</sup> Victor R. Gordeuk,<sup>4</sup> Mark T Gladwin<sup>6,\*</sup>

- 1) Department of Biochemistry and Molecular Genetics, University of Colorado Denver – Anschutz Medical Campus, Aurora, CO, USA
- 2) Department of Medicine – Division of Hematology, University of Colorado Denver – Anschutz Medical Campus, Aurora, CO, USA
- 3) Division of Pulmonary, Allergy and Critical Care Medicine, Department of Medicine, University of Pittsburgh, Pennsylvania, USA.
- 4) Department of Medicine, University of Illinois at Chicago, Chicago, Illinois, USA.
- 5) Linda Crnic Institute for Down Syndrome, University of Colorado – Anschutz Medical Campus, Aurora, CO, USA
- 6) University of Maryland School of Medicine, University of Maryland, Baltimore, MD, USA.

### \*Correspondence:

Angelo D'Alessandro, PhD  
Department of Biochemistry and Molecular Genetics  
University of Colorado Anschutz Medical Campus  
12801 East 17th Ave., Aurora, CO 80045  
Phone # 303-724-0096  
E-mail: [angelo.dalessandro@ucdenver.edu](mailto:angelo.dalessandro@ucdenver.edu)

Mark T. Gladwin, MD PhD  
Dean, University of Maryland School of Medicine;  
Vice President for Medical Affairs,  
John Z. and Akiko K. Bowers Distinguished Professor  
University of Maryland, Baltimore, MD, USA  
Phone: # 410-706-7410;  
E-mail: [mgladwin@som.umaryland.edu](mailto:mgladwin@som.umaryland.edu)

### TABLE OF CONTENTS

<b>SUPPLEMENTARY MATERIALS AND METHODS EXTENDED.....</b>	<b>2</b>
<b>SUPPLEMENTARY REFERENCES.....</b>	<b>3</b>
<b>SUPPLEMENTARY FIGURES.....</b>	<b>5</b>
<b>SUPPLEMENTARY FIGURE 1 .....</b>	<b>5</b>
<b>SUPPLEMENTARY FIGURE 2 .....</b>	<b>6</b>
<b>SUPPLEMENTARY FIGURE 3 .....</b>	<b>7</b>
<b>SUPPLEMENTARY FIGURE 4 .....</b>	<b>8</b>
<b>SUPPLEMENTARY FIGURE 5 .....</b>	<b>9</b>
<b>SUPPLEMENTARY FIGURE 6 .....</b>	<b>10</b>
<b>SUPPLEMENTARY FIGURE 7 .....</b>	<b>11</b>
<b>SUPPLEMENTARY FIGURE 8 .....</b>	<b>12</b>
<b>SUPPLEMENTARY FIGURE 9 .....</b>	<b>13</b>
<b>SUPPLEMENTARY FIGURE 10.....</b>	<b>14</b>
<b>SUPPLEMENTARY FIGURE 11.....</b>	<b>15</b>
<b>SUPPLEMENTARY FIGURE 12.....</b>	<b>16</b>
<b>SUPPLEMENTARY DATA TABLE (PLEASE REFER TO “LEGEND” SHEET WITHIN THE FILE).....</b>	<b>XLSX</b>

## *Supplementary Materials and Methods - Extended*

### ***Ultra-High-Pressure Liquid Chromatography-Mass Spectrometry (MS) metabolomics:***

Frozen plasma aliquots (50  $\mu$ L) were thawed on ice then extracted 1:25, in ice cold extraction solution (methanol:acetonitrile:water 5:3:2 v/v/v). Samples were vortexed for 30 min at 4°C and insoluble material pelleted via centrifugation at 15,000 g for 15 min under refrigerated conditions, as described.<sup>1,2</sup> Analyses were performed using a Vanquish UHPLC coupled online to a Q Exactive mass spectrometer (Thermo Fisher, Bremen, Germany). Samples were resolved as described,<sup>3,4</sup> over a Kinetex C18 column (2.1x150 mm, 1.7  $\mu$ m; Phenomenex, Torrance, CA, USA) at 45°C. A volume of 10  $\mu$ L of sample extracts was injected into the UHPLC-MS. Each sample was injected with two different chromatographic and MS conditions as follows: 1) using a 5 minute gradient at 450  $\mu$ L/minute from 5-95% B (A: water/0.1% formic acid; B:acetonitrile/0.1% formic acid) and the MS was operated in positive mode and 2) using a 5 minute gradient at 450  $\mu$ L/minute from 5-95% B (A: 5% acetonitrile, 95%water/1 mM ammonium acetate; B:95%acetonitrile/5% water, 1 mM ammonium acetate) and the MS was operated in negative ion mode. The UHPLC system was coupled online with a Q Exactive scanning in Full MS mode at 70,000 resolution in the 60-900 m/z range, 4 kV spray voltage, 15 sheath gas and 5 auxiliary gas. These chromatographic and MS conditions were applied for both relative and targeted quantitative metabolomics measurements, with the differences that for the latter targeted quantitative post hoc analyses were performed on the basis of the stable isotope-labeled internal standards used as a reference quantitative measurement, as detailed below.

***Quality control and data processing:*** Calibration was performed prior to analysis using the Pierce<sup>TM</sup> Positive and Negative Ion Calibration Solutions (Thermo Fisher Scientific). Acquired data was then converted from raw to .mzXML file format using RawConverter. Samples were analyzed in randomized order with a technical mixture injected every 15 samples to qualify instrument performance and ensure technical coefficients of variations (standard deviation divided by the mean) below 20%. Metabolite assignments, isotopologue distributions, and quantification of stable isotope-labeled internal standards were performed using MAVEN (Princeton, NJ, USA), as described.<sup>5</sup>

***Statistical analyses:*** Data analysis was performed through the auxilium of the software MAVEN. Graphs and statistical analyses (either two-way ANOVA or repeated measures

ANOVA) were prepared with GraphPad Prism 9.0 (GraphPad Software, Inc, La Jolla, CA), GENE E (Broad Institute, Cambridge, MA, USA), Multivariate analyses, including principal component analyses (PCA), hierarchical clustering analyses, two-way ANOVAs, correlation analyses (Spearman) and calculation of receiver operating characteristic (ROC) curves were performed through the software MetaboAnalyst 5.0.<sup>6</sup> For survival analysis, we used time to right censorship (including death or last follow-up) as time to event and vital status (death or alive) was the studied outcome. PCA was used to derive a hemolytic component from lactate dehydrogenase, aspartate aminotransferase total bilirubin and reticulocyte percent.<sup>7-9</sup> We applied Cox proportional hazard models to calculate the hazard ratios and P value for each metabolite. and Cox analysis and adjusted regressions of metabolites to clinical outcomes were performed in R (R Core Team (2022), <https://www.r-project.org/>).

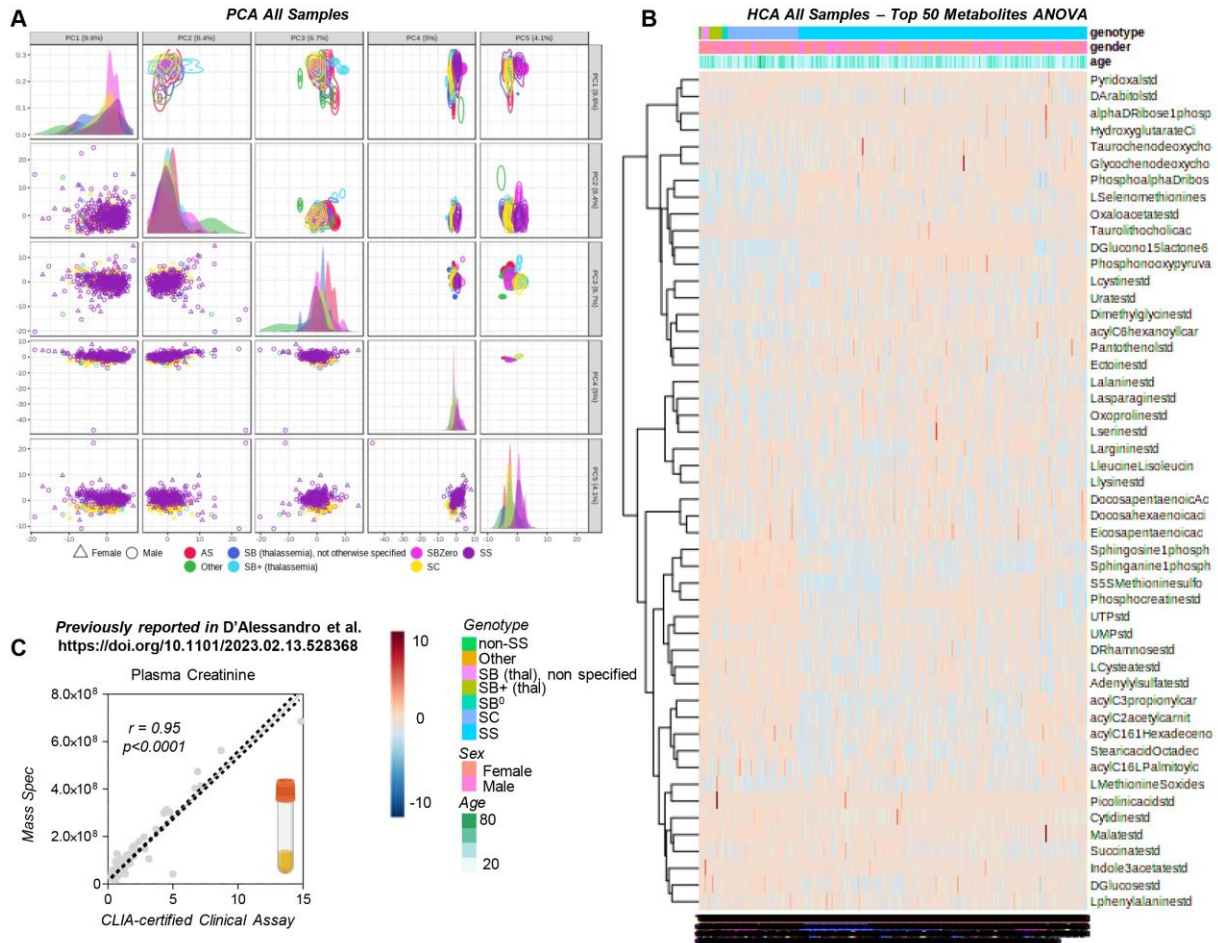
***Sickle Cell Disease ShinyApp portal*** A portal for online sharing of all the data generated in this study, in like-wise fashion to our recent COVID-Ome Explorer portal.<sup>10</sup> After data curation and quality control, each of the datasets (plasma metabolomics, RBC metabolomics from our previous study on the WALK-PHASST Cohort<sup>11</sup>, clinical data) was linked at the sample level with a unique identifier, enabling cross-referencing among datasets. Then, each of the datasets was imported into applications developed using R, R Studio, and the R-based web application framework Shiny. All code required to run the COVIDome Explorer applications can be found at <https://github.com/cusom/CUSOM.COVIDome.Shiny-Apps> (Zenodo <https://doi.org/10.5281/zenodo.5081091>) and <https://github.com/cusom/CUSOM.ShinyHelpers> (Zenodo <https://doi.org/10.5281/zenodo.5081093>).

### Supplementary references

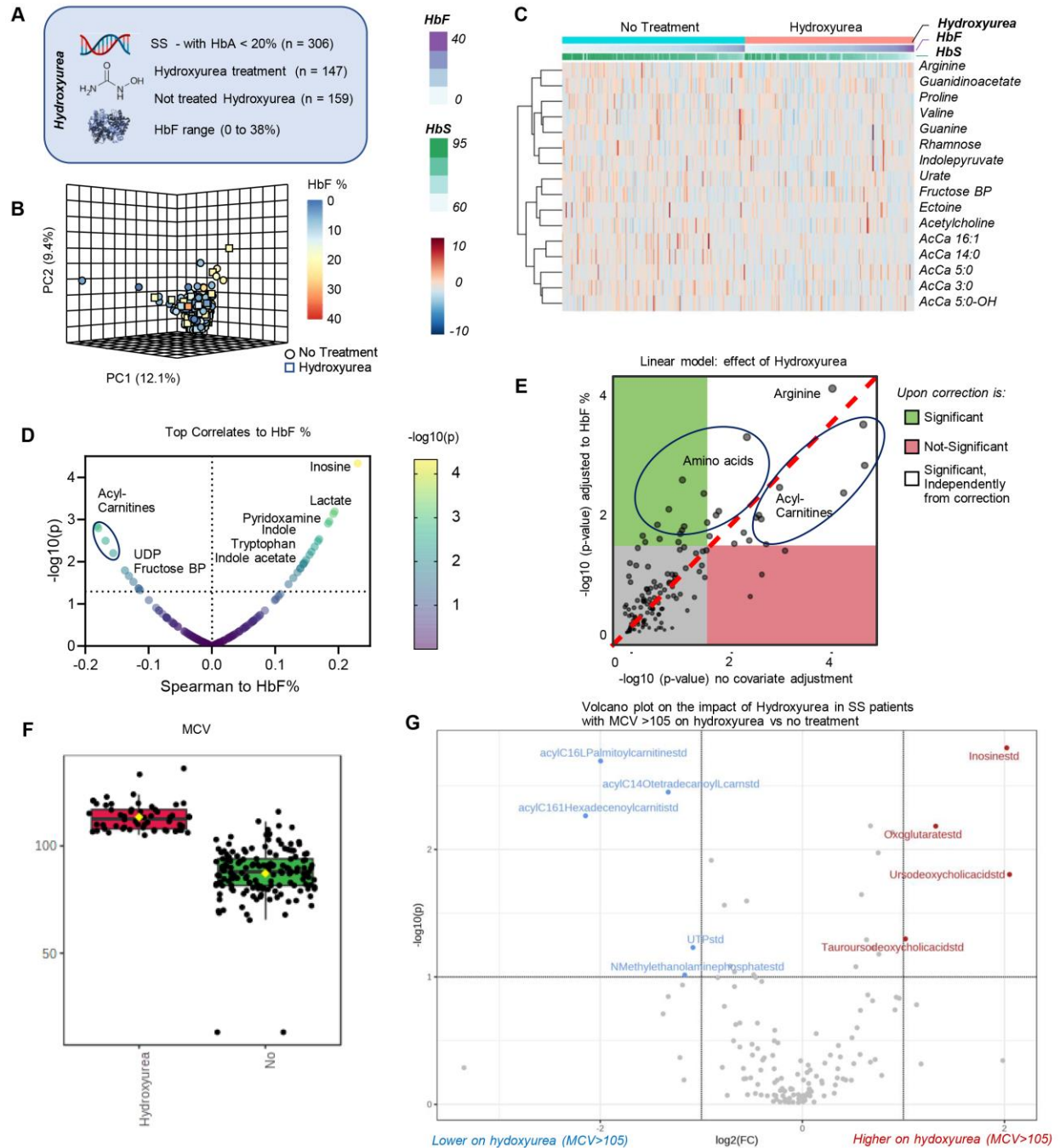
1. Bertolone L, Shin HK, Stefanoni D, et al. ZOOMICS: Comparative Metabolomics of Red Blood Cells From Old World Monkeys and Humans. *Front Physiol.* 2020;11:593841.
2. Stefanoni D, Shin HKH, Baek JH, et al. Red blood cell metabolism in Rhesus macaques and humans: comparative biology of blood storage. *Haematologica.* 2020;105(8):2174-2186.
3. Nemkov T, Hansen KC, D'Alessandro A. A three-minute method for high-throughput quantitative metabolomics and quantitative tracing experiments of central carbon and nitrogen pathways. *Rapid Commun Mass Spectrom.* 2017;31(8):663-673.

4. Nemkov T, Reisz JA, Gehrke S, Hansen KC, D'Alessandro A. High-Throughput Metabolomics: Isocratic and Gradient Mass Spectrometry-Based Methods. *Methods Mol Biol.* 2019;1978:13-26.
5. D'Alessandro A, Culp-Hill R, Reisz JA, et al. Heterogeneity of blood processing and storage additives in different centers impacts stored red blood cell metabolism as much as storage time: lessons from REDS-III-Omics. *Transfusion.* 2019;59(1):89-100.
6. Pang Z, Chong J, Zhou G, et al. MetaboAnalyst 5.0: narrowing the gap between raw spectra and functional insights. *Nucleic Acids Research.* 2021;49(W1):W388-W396.
7. Minniti CP, Sable C, Campbell A, et al. Elevated tricuspid regurgitant jet velocity in children and adolescents with sickle cell disease: association with hemolysis and hemoglobin oxygen desaturation. *Haematologica.* 2009;94(3):340-347.
8. Nourai M, Lee JS, Zhang Y, et al. The relationship between the severity of hemolysis, clinical manifestations and risk of death in 415 patients with sickle cell anemia in the US and Europe. *Haematologica.* 2013;98(3):464-472.
9. Page GP, Kaniyas T, Guo YJ, et al. Multiple-ancestry genome-wide association study identifies 27 loci associated with measures of hemolysis following blood storage. *J Clin Invest.* 2021;131(13).
10. Sullivan KD, Galbraith MD, Kinning KT, et al. The COVIDome Explorer researcher portal. *Cell Reports.* 2021;36(7):109527.
11. D'Alessandro A, Nourai M, Zhang Y, et al. In vivo evaluation of the effect of sickle cell hemoglobin S, C and therapeutic transfusion on erythrocyte metabolism and cardiorenal dysfunction. *Am J Hematol.* 2023; doi: 10.1002/ajh.26923

## SUPPLEMENTARY FIGURES

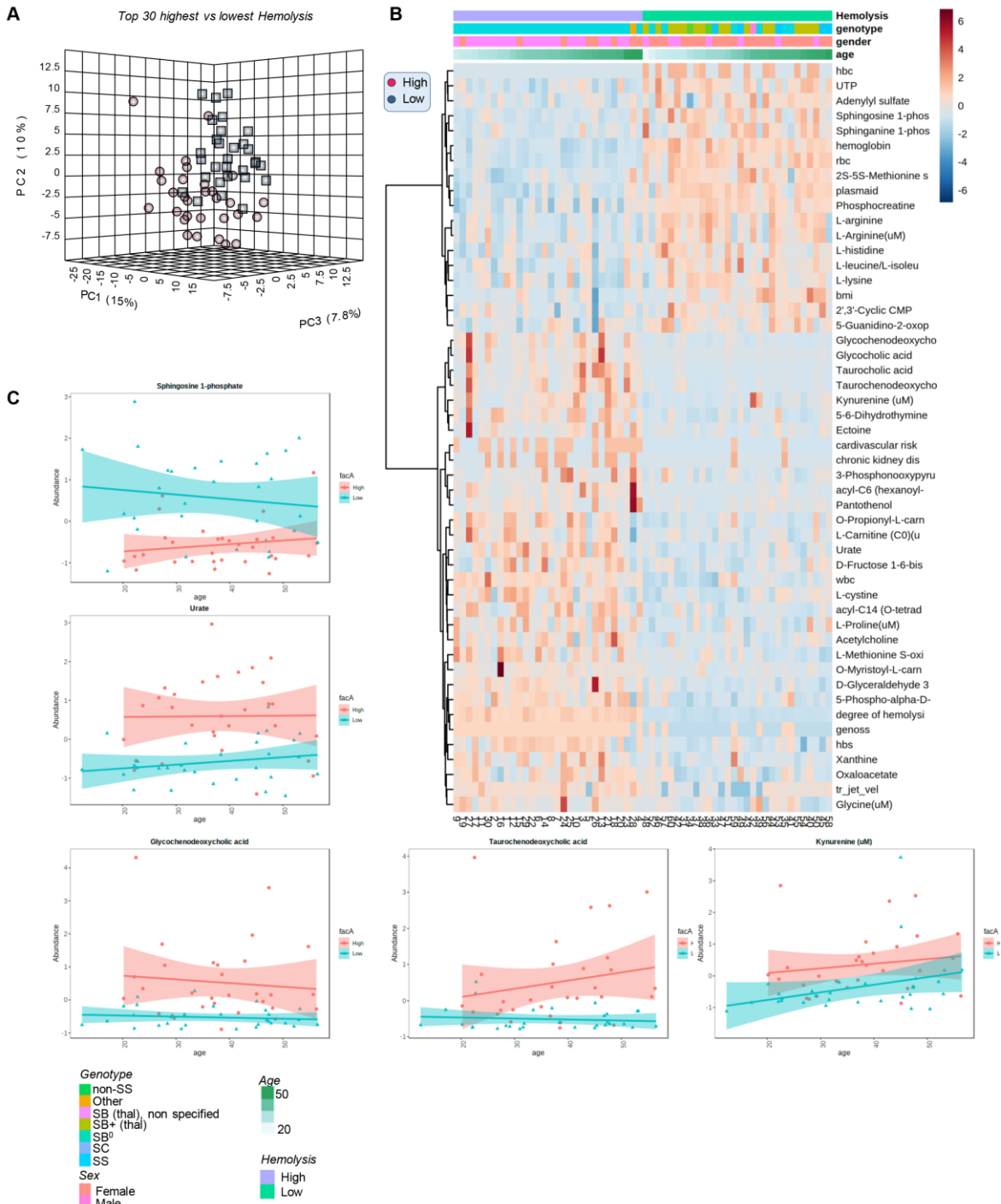


**Supplementary Figure 1 Plasma metabolomics of the WALK-PHASST SCD cohort** Principal component analysis (PCA) (A) and hierarchical clustering analysis (B) of metabolomics data on 596 plasma samples from 6 different genotypes. Of note, metabolomics measurements of plasma creatinine showed significant positive correlation ( $r=0.95$ ) with CLIA-measurements in the clinics, despite double randomization of the samples, blinding of the mass spec lab and prolonged storage of the Walk-PHASST samples (C), as previously noted.<sup>11</sup>



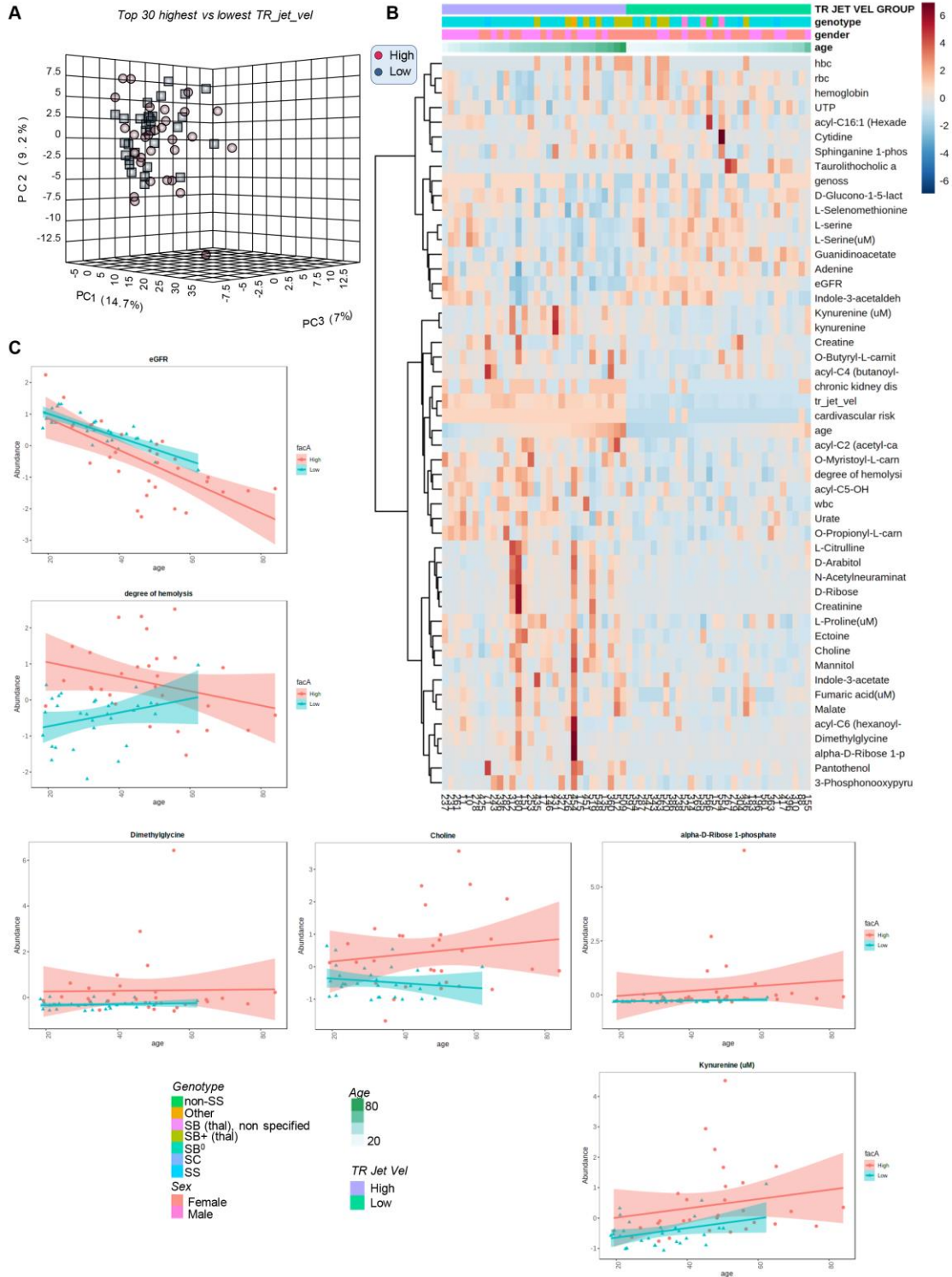
**Supplementary Figure 2 Plasma metabolic correlates to Hydroxyurea treatment in the WALK-PHaSST cohort** SS patients who were not recently transfused (HbA < 20%; n = 306) were tested as a function of treatment with hydroxyurea (n = 147 vs n = 159 untreated - **A**). In **B**, principal component analysis of the data from this cohort, color-coded based on HbF %. In **C**, heat map of the most significant metabolites affected by the treatment. In **D**, metabolic correlates to HbF%. In **E**, linear model identifying the effect of hydroxyurea in SS patients, either unadjusted (x axis) or adjusted by HbF% (y axis). In **F**, to reduce the noise in the hydroxyurea group, owing to questionable adherence to the treatment, we narrowed the analysis down to the patients on

treatment with MCV >105. The analysis (G) showed a beneficial effect of hydroxyurea in lowering the levels of several circulating acylcarnitines, an effect that was masked by the general analysis.

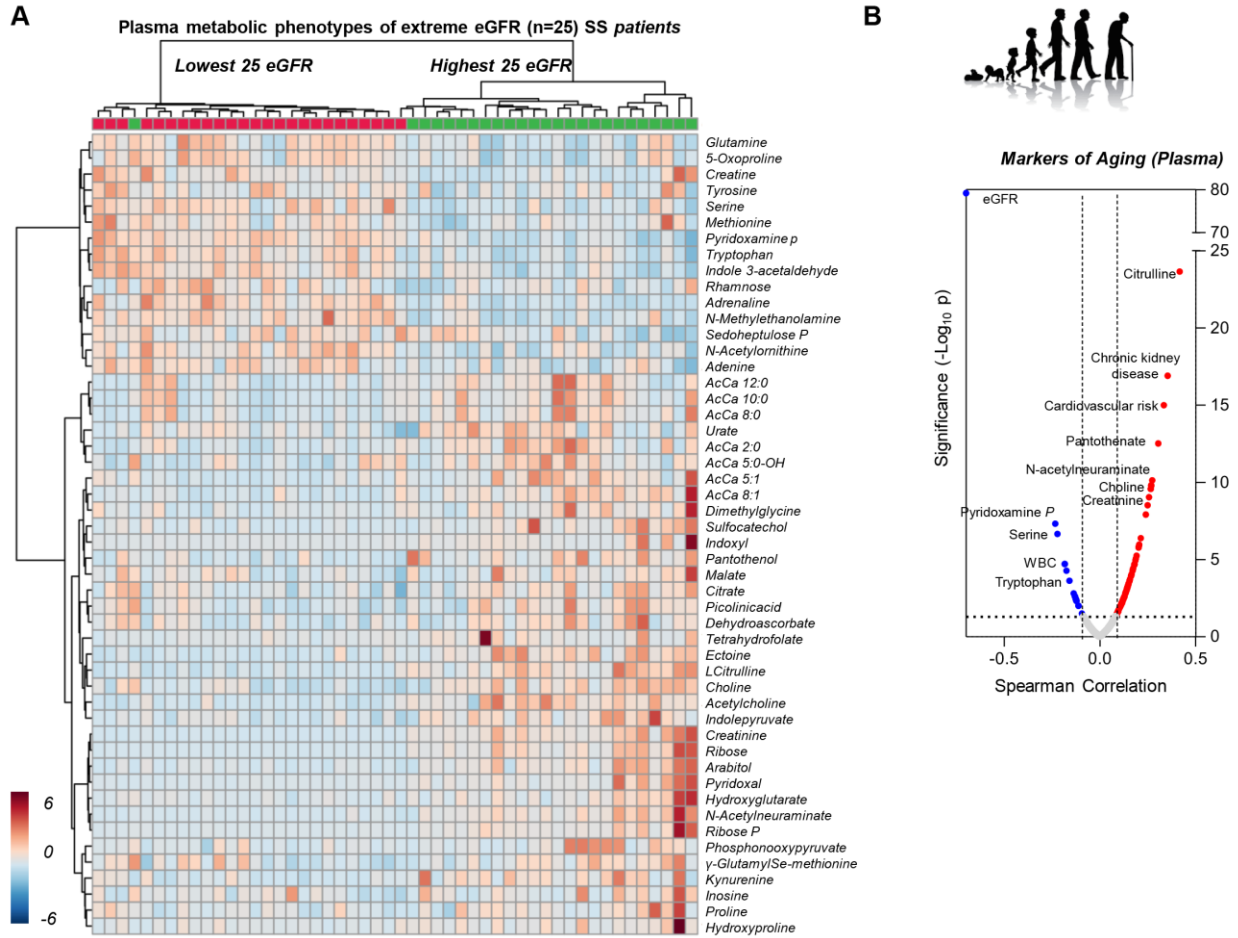


**Supplementary Figure 3** Plasma metabolomics of patients enrolled in the *WALK-PHASST* study with high and low hemolytic propensity tracks with genotypes (high in SS, low in SC) and shows distinct metabolic phenotypes, as gleaned by principal component analysis (A), hierarchical clustering analysis (B) and line plots (C – x axis tracks with patients' age).

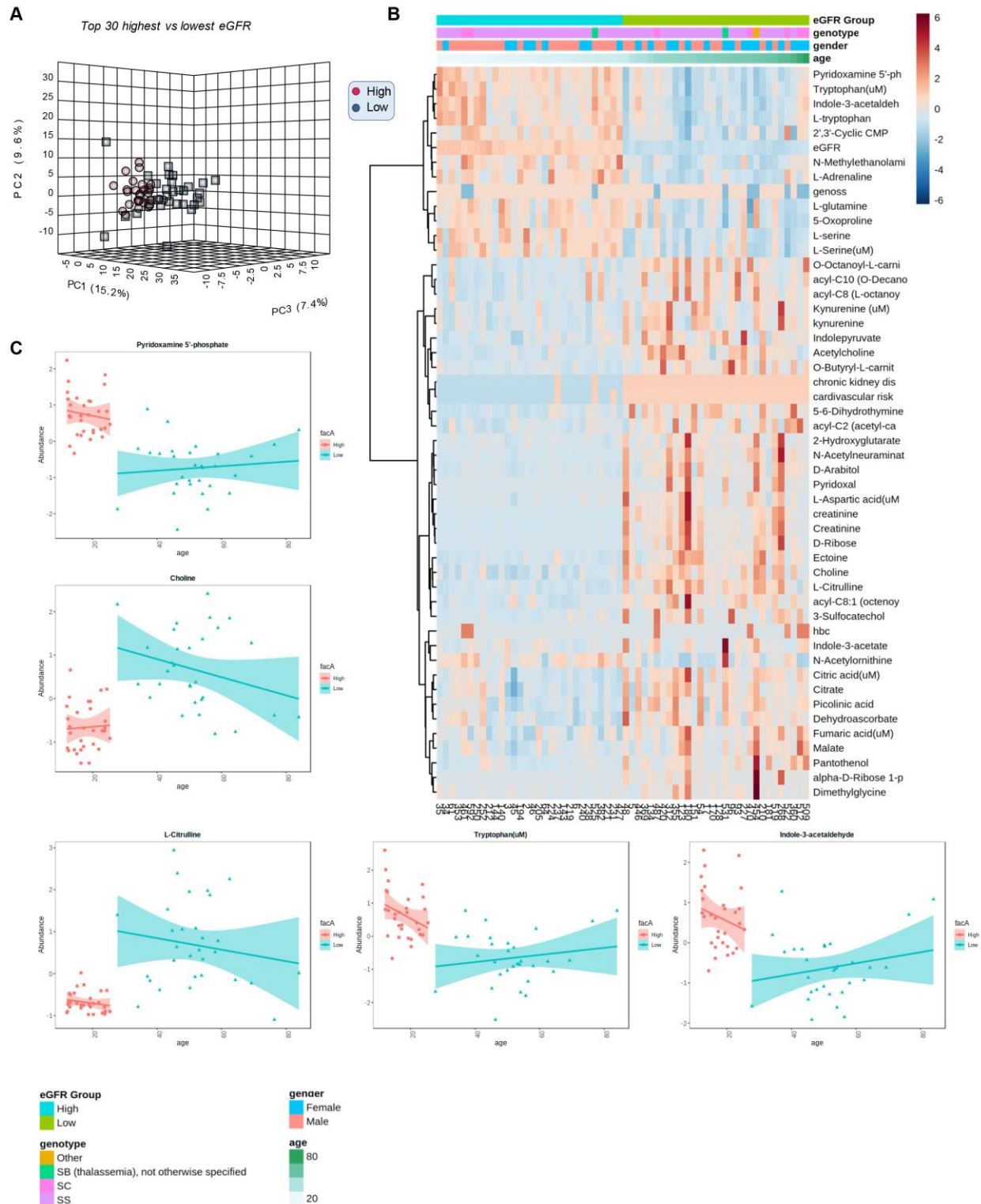




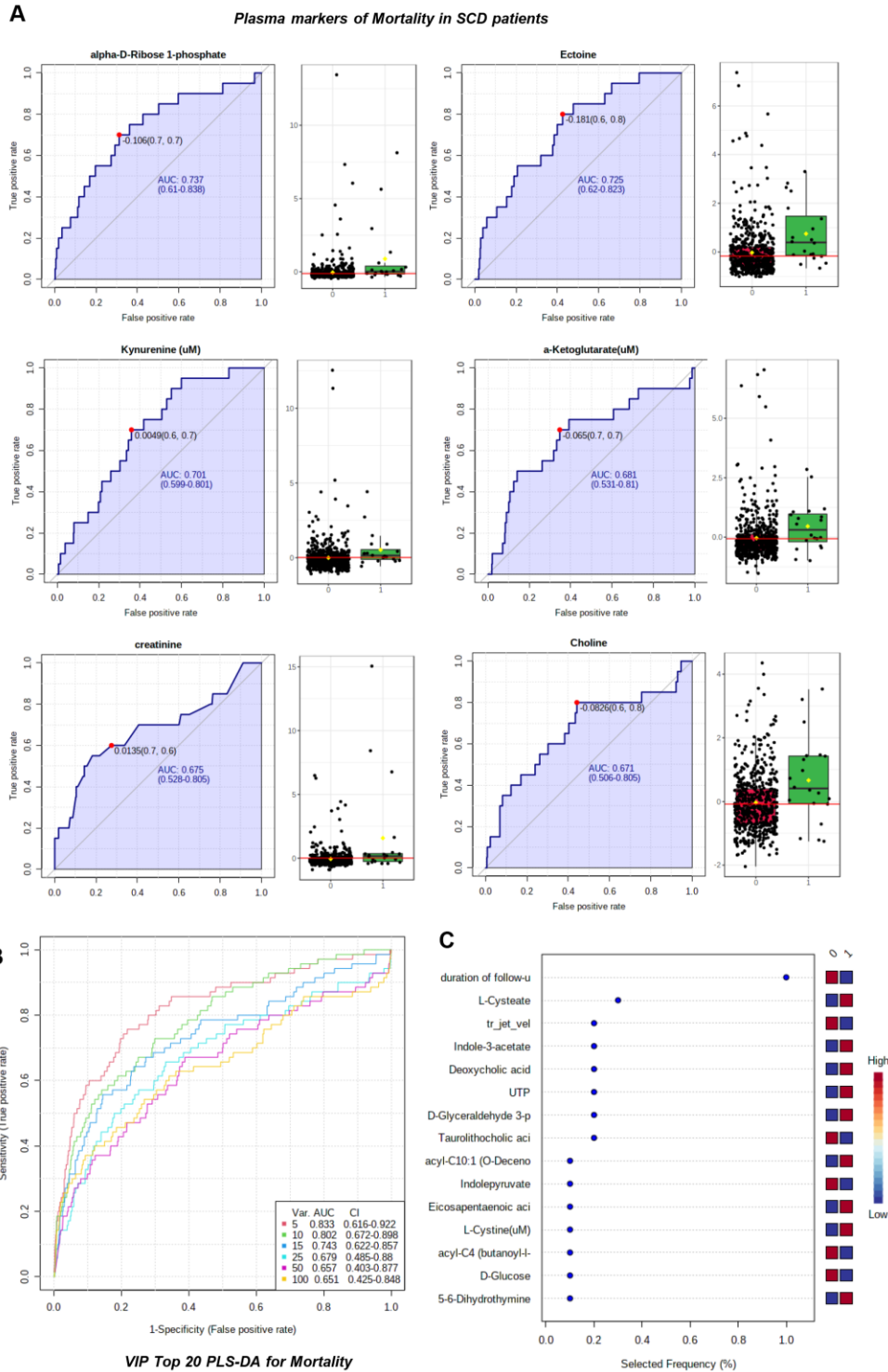
**Supplementary Figure 4 Plasma metabolomics of patients enrolled in the WALK-PHASST study with high and low tricuspid regurgitation velocity (TRV) tracks with genotypes (high in SS, low in SC), age (high in older patients) and shows distinct metabolic phenotypes, as gleaned by principal component analysis (A), hierarchical clustering analysis (B) and line plots (C – x axis tracks with patients' age).**



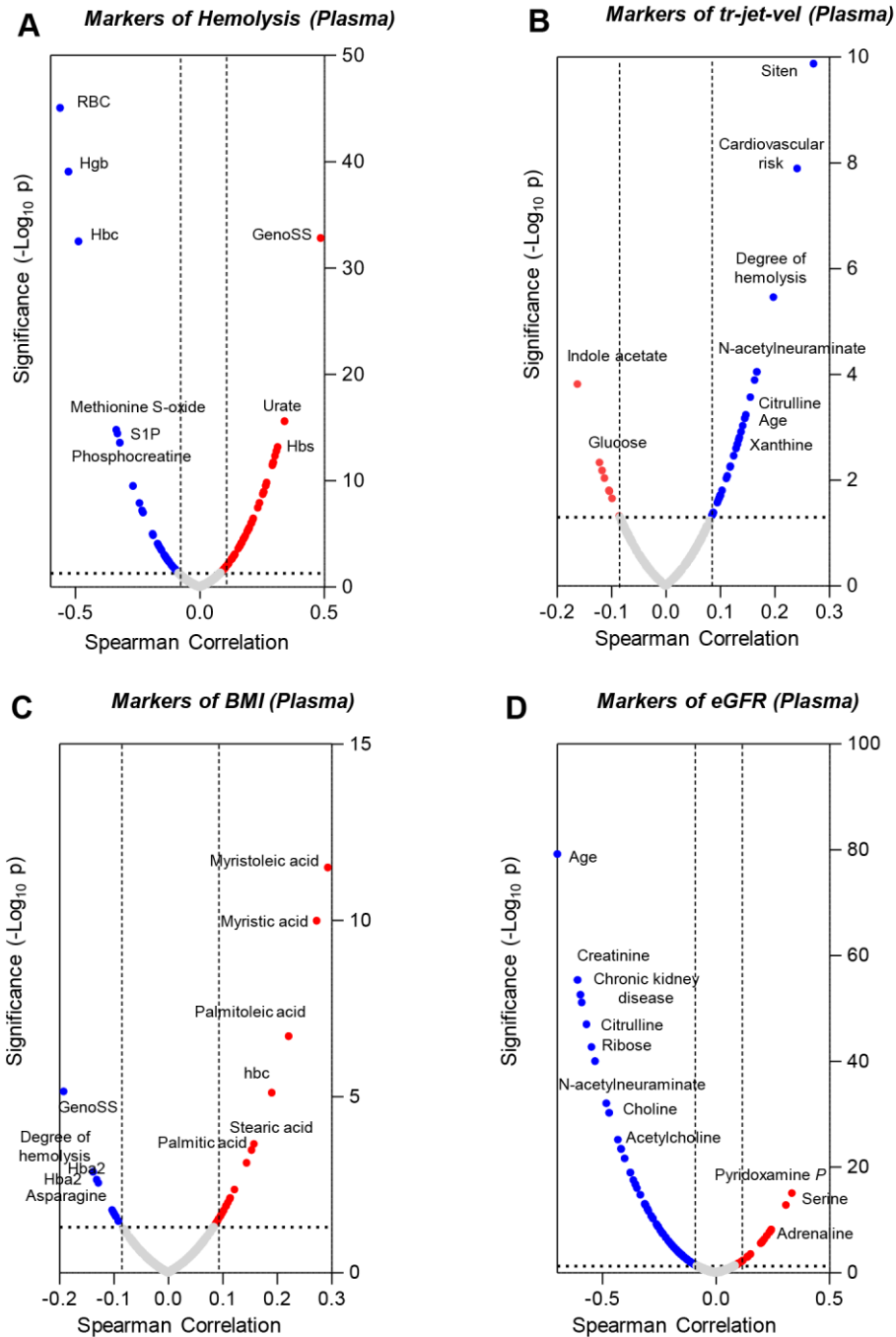
**Supplementary Figure 5** Plasma metabolomics of patients enrolled in the WALK-PHASST study with high and low eGFR propensity, as gleaned by hierarchical clustering analysis (A). Metabolic markers and clinical measurements of kidney dysfunction were identified as the top correlates to patients' age (Spearman - B).



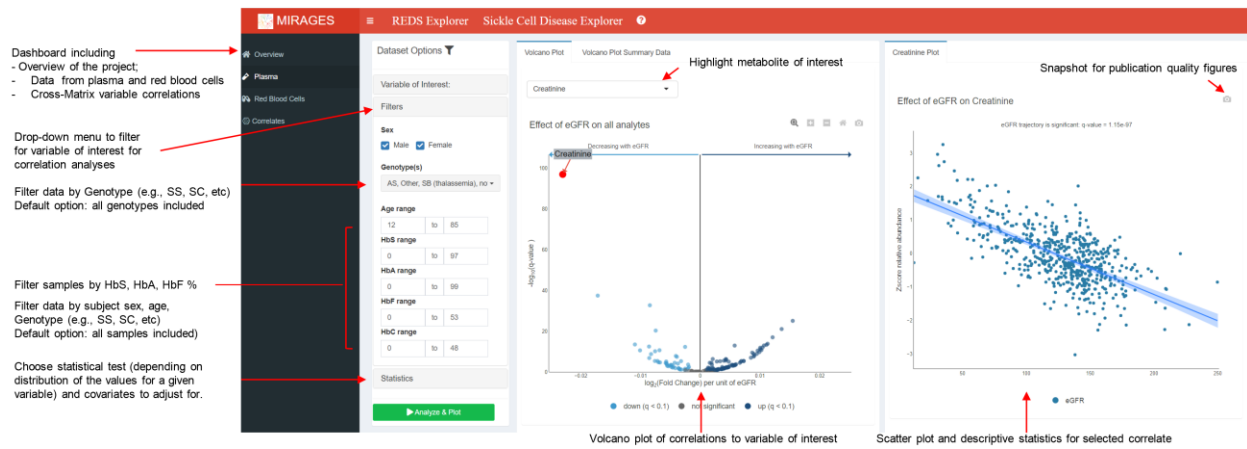
**Supplementary Figure 6** *Plasma metabolomics of patients enrolled in the WALK-PHASST study with high and low eGFR tracks with genotypes (high in SC, low in SS) and shows distinct metabolic phenotypes, as gleaned by principal component analysis (A), hierarchical clustering analysis (B) and line plots (C – x axis tracks with patients' age).*



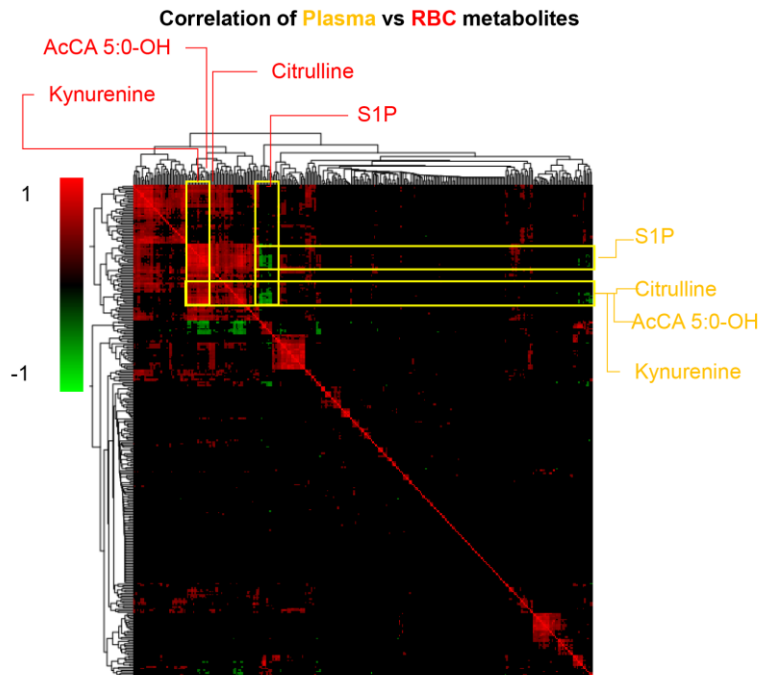
**Supplementary Figure 7 Plasma metabolic markers of mortality** as determined by receiver operating characteristic curves (ROC – **A**), multivariate analyses via random forest (**B**). The top 15 variables from this analysis are reported in **C**.



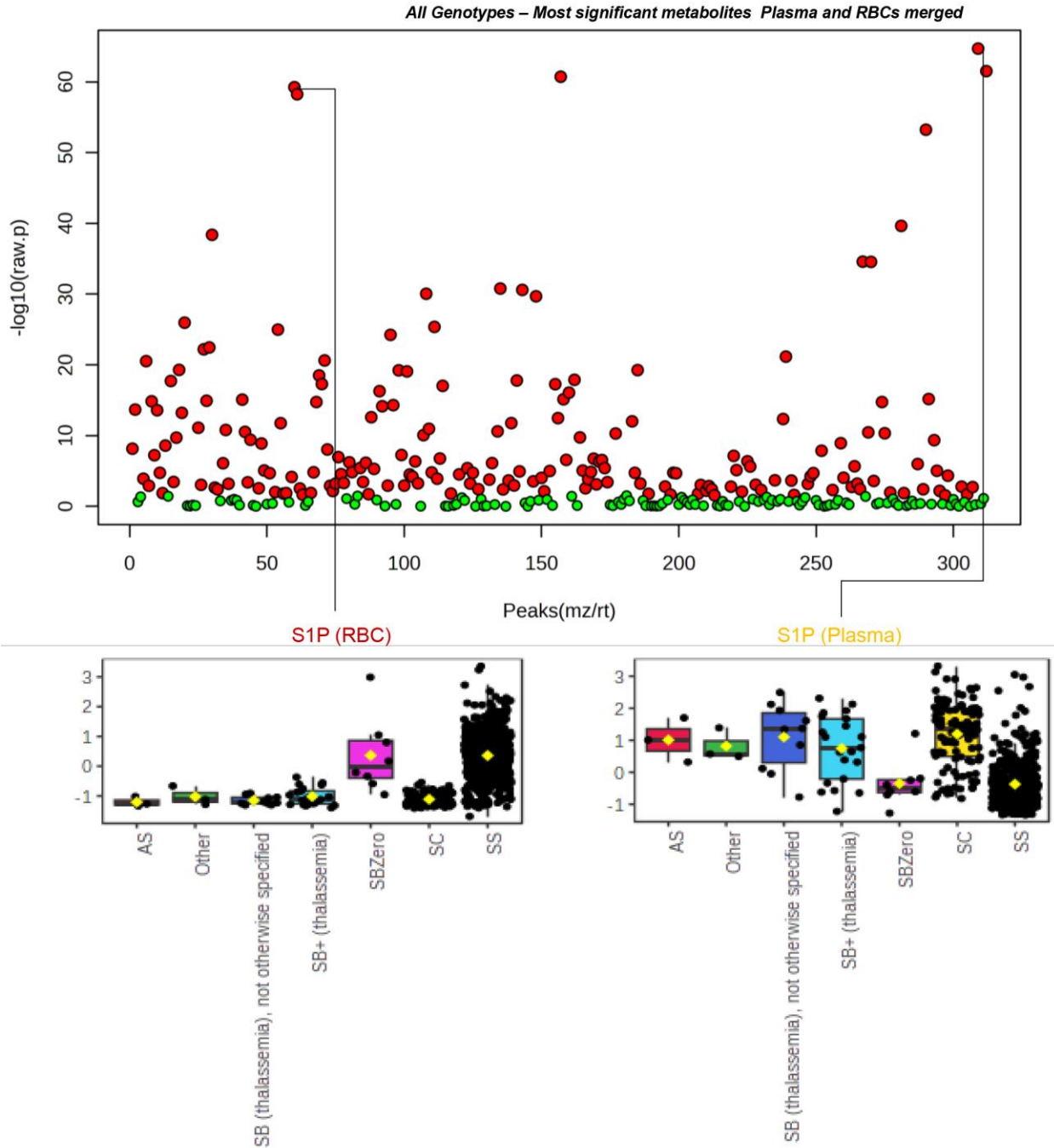
**Supplementary Figure 8 Plasma metabolomics correlates to clinical and hematological parameters**, including the degree of hemolysis (A), TRV (B), body mass index (BMI – C), estimated glomerular filtration rate (eGFR - D).



**Supplementary Figure 9 Overview of the MIRAGES Sickle Cell Disease portal** which offers the opportunity to perform streamlined data analysis of plasma, red blood cells or cross-matrix analyses of metabolomics data as a function of relevant clinical or hematological covariates, patients' demographics data. The portal is freely accessible at: <https://mirages.shinyapps.io/SickleCellDisease/>

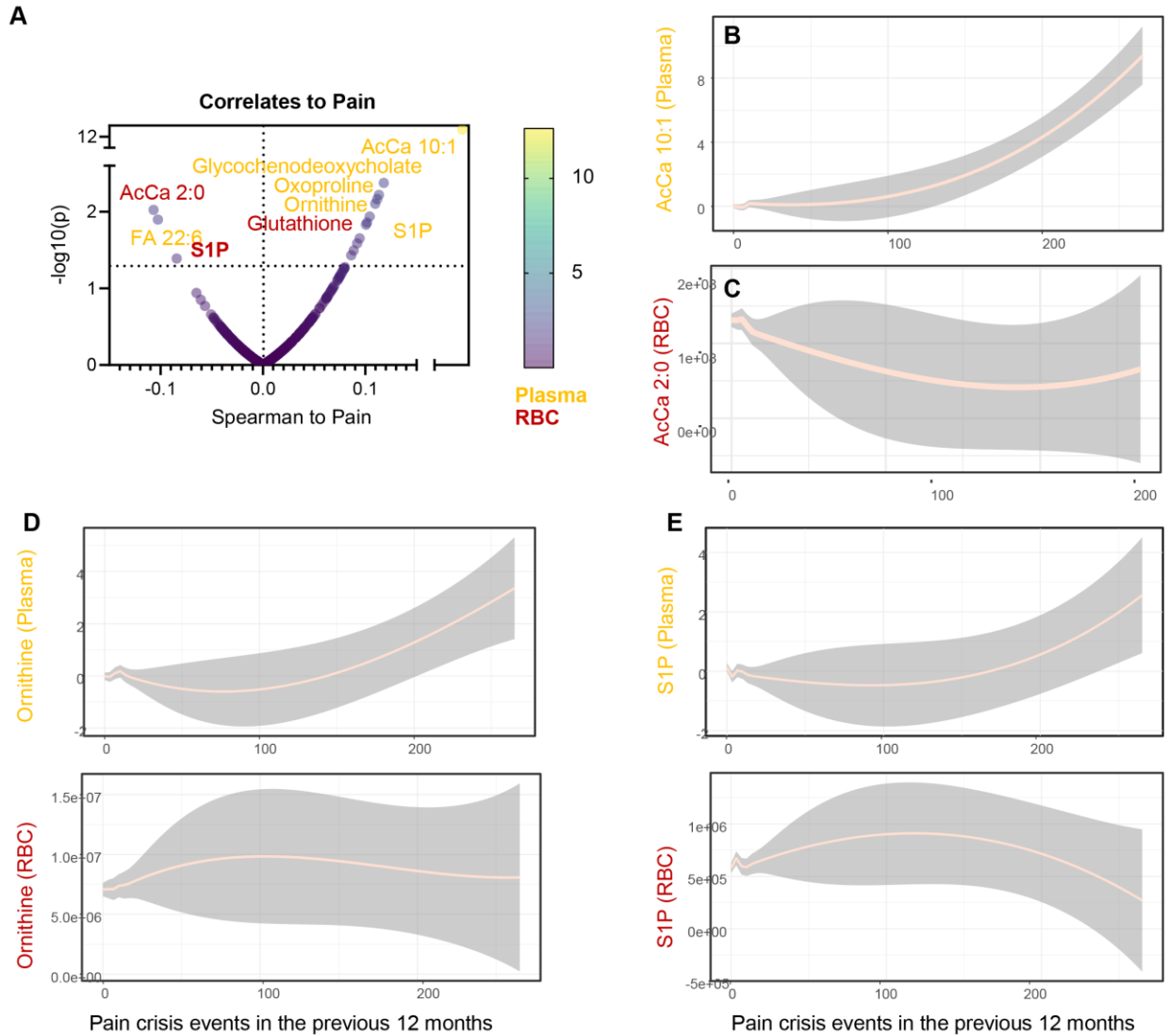


**Supplementary Figure 10 Plasma vs RBC metabolites: correlation matrix** Plasma metabolite levels from the WALK PHASST cohort were matched to RBC metabolomics measurements (*D'Alessandro et al. Am J Hematol 2023<sup>21</sup>*). Results indicated a strong positive cross-matrix correlation for almost all metabolic markers of cardiorenal dysfunction, except for sphingosine 1-phosphate (S1P), whose levels were elevated in SS RBCs and SC plasma, suggesting an increased synthesis or decreased export in the more clinically severe SS genotype



**Supplementary Figure 11 ANOVA of merged metabolomics data from plasma and red blood cells from our recent Walk-PHASST study.<sup>11</sup>** Determination of the most significantly impacted metabolites in plasma (present study) and RBCs<sup>11</sup> from the Walk-PHASST trial are shown in the Manhattan plot at the top of the figure, where the y axis indicates  $-\log_{10}$  of p-values by ANOVA based on patients' genotypes and HbS%. Of note, sphingosine 1-phosphate (S1P) in plasma and RBC ranked amongst the top 5 most significantly impacted metabolites of both matrices, though its levels were higher in SS RBCs and lower in SS plasma compared to other genotypes (box plots at the bottom of the figure).





**Supplementary Figure 12 Plasma and RBC metabolic correlates to pain crisis events in SCD**

Spearman correlation of plasma (yellow) and RBC (red) metabolite levels to self-reported pain crisis events in the 12 months preceding the analysis (A). Line plots show (Loess smoothing algorithm-adjusted) median ( $\pm$  quartile) associations to pain for AcCa 10:1, 2:0, ornithine and S1P in plasma and RBC (B-E).